Aust. Met. Mag. 47 (1998) 191-202

The relationship between maximum surface wind speeds and central pressure in tropical cyclones

Jeff Callaghan
Regional Office, Bureau of Meteorology, Brisbane, Australia
and
Roger K. Smith
Meteorological Institute, University of Munich, Germany

(Manuscript received February 1997; revised October 1997)

The central surface pressure of a tropical cyclone has long been used as an indication of its intensity. There have been occurrences when unexpected high (low) maximum surface wind speeds have been associated with relatively high (low) central surface pressures. In this study we have sought to identify situations when, on the basis of established empirical relationships, the central surface pressure of a tropical cyclone misrepresents its maximum wind speed and show examples of cyclones for which this is the case. It appears that the largest discrepancies occur in the case of small or large tropical cyclones and in the case of fast-moving storms. We present simple theoretical arguments in support of these observations, which, to the extent that storms are axisymmetric and in gradient-wind balance, are in line with elementary dynamical considerations.

Introduction

Historically the users of the Tropical Cyclone Warning Centres' products in Australia take the central mean sea-level (MSL) pressure* of a tropical cyclone as a gauge of its intensity. Shea and Gray (1973) showed that, on average, the central pressure is negatively correlated with the maximum wind speed. However, their scatter diagram indicates a large variation in maximum winds at various central pressures. An easy approach to avoid confusion would be to remove the mention of central pressure in warnings and bulletins. This would undoubtedly provoke a negative response from users, many of whom relate central pressure to intensity. There are several arguments for retaining the mention of central pressure on warnings. One is that they often do provide a good guide to the intensity of a cyclone. The experience in the northeastern Australia region is that pressure observations are more likely to be received from the eye of a cyclone than wind observations near the eyewall.

Corresponding author address: Mr J. Callaghan, Bureau of Meteorology, GPO Box 413, Brisbane, Qld 4001, Australia.

* Henceforth referred to as the 'central pressure'.

The aim of this paper is to attempt to identify particular tropical cyclone structures and periods in their life cycles when there are large departures from a general relationship. The relationship between the central pressure and the maximum 10-minute mean wind (10 m above a smooth surface with roughness length approximately 0.01 m) that has been used in recent years in the Queensland Tropical Cyclone Warning Centre is shown in Table 1. At selected values of central pressure, these winds are compared with several other relationships between central pressure and maximum wind speed. Column A lists the Atlantic 900 hPa reconnaissance flight level maximum winds along the line of best fit in the scatter diagram from Shea and Gray (1973). Column B lists the maximum sea-surface winds, estimated from reconnaissance flight sea-state photographs, and the corresponding central pressure from a linear best fit for northwest Pacific tropical cyclones (Subbaramayya and Fujiwhara 1979). Columns C and D are the operational maximum one-minute winds used in the Atlantic and northwest Pacific respectively.

Table 1. Comparison of relationships between central pressure and maximum wind speed (knots with m s^{-1} in brackets) in three tropical cyclone basins with aircraft reconnaissance data at 900 hPa over the Atlantic (Shea and Gray 1973) and at 10 m over the northwest Pacific (Subbaramayya and Fujiwhara 1979).

Central pressure (hPa)	*Brisbane TCWC 10-min winds*	*A Atlantic 900 hPa winds*	*B Northwest Pacific 10 m winds*	*C 1 min Atlantic*	*D 1 min Northwest Pacific*
980	55	68	56	75	60
	(28)	(35)	(29)	(39)	(31)
970	65	73	67	90	72
	(34)	(38)	(35)	(46)	(37)
960	75	78	76	102	83
	(39)	(40)	(39)	(53)	(43)
950	83	87	85	113	94
	(43)	(45)	(44)	(58)	(48)
940	87	100	95	122	103
	(45)	(51)	(49)	(63)	(53)
930	95	115	105	132	112
	(49)	(59)	(54)	(68)	(58)
920	108	132	115	140	122
	(56)	(68)	(59)	(72)	(63)

We examine a number of cases in which the central pressure of a tropical cyclone misrepresented the maximum wind speed. Although the scope falls short of a climatological study, we have found that the largest discrepancies occur in the case of large or small tropical cyclones and in the case of fast-moving storms. We present theoretical arguments to explain these observations, and show that to the extent that storms are axisymmetric and in gradient-wind balance, the observations are supported by simple dynamical considerations.

Tropical cyclone size

Several intense and extremely small tropical cyclones have been observed in the Australian region. From the available observations it has been suspected that they have higher central pressures than larger storms of the same intensity (i.e. maximum wind speed). In addition, very large cyclones with large ragged eyes have been suspected of having lower central pressures than average-sized storms of the same intensity. Data from two tropical cyclones which made landfall along the east coast of Australia with almost identical central pressures showed they were extremely different in size and in impact. It was this discrepancy that motivated the first author to initiate this study and the two cyclones in question are compared below in detail. Other cyclones of varying sizes are also examined, including some from the northern hemisphere. Further, we present simple theoretical arguments which show that for a given storm intensity, the central pressure decreases as the storm size increases, as measured by the scale of its outer circulation.

Large tropical cyclones

In the northeastern Australian region a tropical cyclone is considered large if the gale-force winds (10-minute average wind speeds of more than 17 m s^{-1}) extend beyond 500 km from the centre on both the equatorial and poleward sides of the cyclone. Figure 1 shows the tracks of the largest known severe tropical cyclones to affect the northeastern Australian region since 1954. These all originated well out in the Pacific east of Vanuatu. Large tropical cyclones in the north Atlantic and northwest Pacific are more likely to occur late in the season (Merrill 1984; Brand 1972). However, the six storms in Fig. 1 are evenly distributed through the season (two each in January, February and March). These southwest Pacific cyclones were very large by world standards. Cyclone *David* had an areal extent of gales larger than that of Atlantic hurricane *Gilbert* (1988). According to Eyre (1989), *Gilbert* was the largest hurricane to have been observed in the Caribbean. Cyclone *David* was of similar size to typhoon *Tip* (1979), described by Dunnavan and Diercks (1980) as possessing the largest surface circulation ever observed in a tropical cyclone. We consider briefly the case of tropical cyclone *Agnes* (1956).

Fig. 1 **Tracks of large tropical cyclones in the southwest Pacific Ocean.**

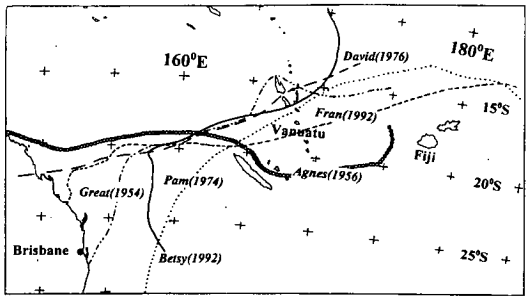

Fig. 2 **Mean sea-level pressure distribution while tropical cyclone *Agnes* was over Townsville.**

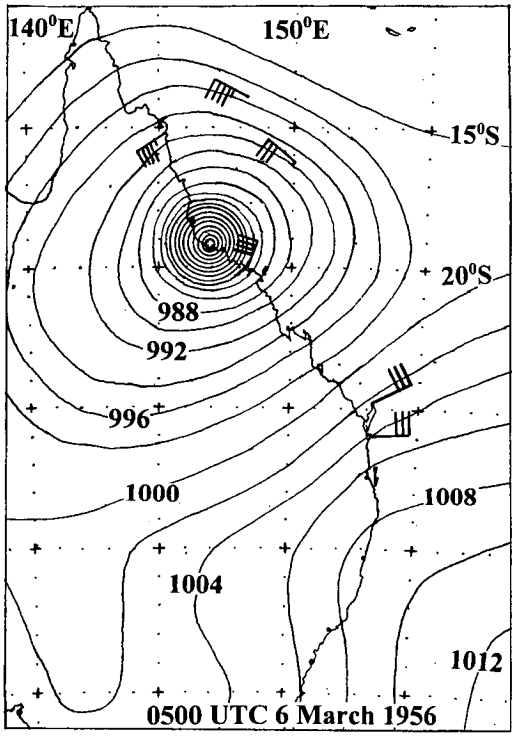

***Agnes* (1956).** Tropical cyclone *Agnes* was a large system with closed isobars covering much of northeastern Australia (Fig. 2) and gales extending more than 500 km from the centre. The eye passed directly over Townsville (2 on map in Fig. 3) which is the largest population centre in tropical Australia. The eye of the cyclone passed directly over the Townsville Meteorological Office and a minimum pressure of 961 hPa was recorded. The eye also passed over two other nearby centres and similar central pressures were recorded. These were 962 hPa at Ayr (4 in Fig. 3) and 959 hPa at Cape Cleveland (3 in Fig. 3). Typical reported damage from all centres in the path of the cyclone were, roofing iron torn off and small sheds blown over. The anemometers from both Townsville (2 in Fig. 3) and Cairns (1 in Fig. 3) Meteorological Offices are shown in Fig. 4. Townsville in those days was a city of just over 40 000 inhabitants and the damage there, though widespread, was mostly relatively minor. However there was some severe damage and the region near the meteorological office was one of the areas affected worst. In all, several days after the event, some 15 to 20 families were still homeless. Interestingly the damage at Cairns was comparable even though the cyclone passed well to the south. Some reports had the damage at Cairns greater than that at Townsville. Close examination of Fig. 4 shows that the maximum gust at Cairns was 79 knots (41 m s^{-1}) while that at Townsville was 73 knots (38 m s^{-1}). The winds at Cairns were phenomenally gusty and gusts exceeded 60 knots (31 m s^{-1}) for a much longer period than at Townsville. As the cyclone passed over Townsville observers estimated the eye diameter to be 28 km. The deep convection, heavy rain and strongest winds were confined to the western side of the eye.

In summary, tropical cyclone *Agnes* was a large storm and produced moderate damage over an extensive area of the northeastern Australian coast. By the time it reached Townsville its inner ring of convective rain was decaying and the peak intensity wind gusts began extending out to large radii. This was particularly evident on the northern side where westerly winds caused widespread damage in the lee of the elevated terrain.

***Gilbert* (1988).** As mentioned above, *Gilbert* was a huge storm. Aircraft reconnaissance data revealed different relationships between central pressure and intensity during its lifetime. The maximum flight level (700 hPa) wind speed recorded in hurricane *Gilbert* was 77 m s^{-1} when its central pressure was 903 hPa (Black and Willoughby (1992); referred to below as BW). *Gilbert's* central pressure was 967 hPa on a flight ending at 2002 UTC 11 September 1988, when the tangential wind maximum was 46 m s^{-1} (Fig. 4(a) in BW). The storm had a peaked wind speed profile radially, with the wind speed maximum associated with an almost complete radar eyewall rain echo (Fig. 3 (b) in BW). Later, an outer eyewall convective ring formed and *Gilbert* underwent the concentric eye cycle which is characteristic of the more intense tropical cyclones (Willoughby 1990a).

Fig. 3 **Position of tropical cyclone *Agnes* every two hours from 1600 UTC 5 March to 1200 UTC 6 March 1956 denoted by cyclone symbols. Locations with numbers are referred to in text. Light (heavy) hatched areas indicate elevations above 300 m (600 m). Over ocean latitude and longitude are marked each degree.**

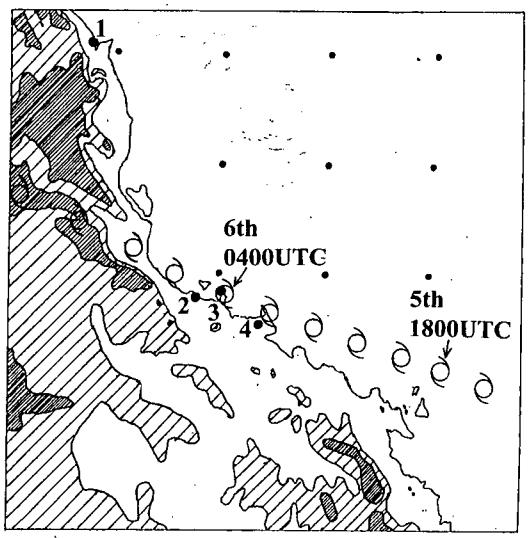

Fig. 4 **Anemograms for Townsville (top) and Cairns (bottom) for 24-hour period 2300 UTC 5 March 1956 to 2300UTC 6 March 1956.**

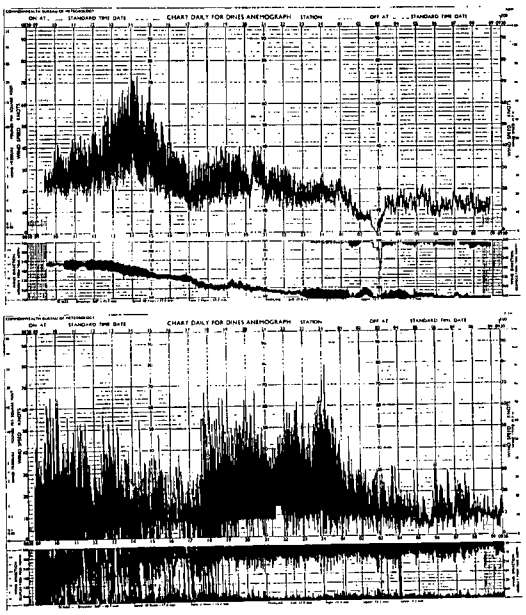

Gilbert's central pressure had risen to 950 hPa by 1204 UTC 15 September 1988, more than one and a half days after reaching peak intensity. From Fig. 4(d) in BW the tangential wind maximum was then less than 40 m s^{-1}. However the radial profile of wind speed was very flat and wind speeds were near 40 m s^{-1} beyond a radius of 150 km. The dominant precipitation feature (Fig. 3 (e) BW) was an outer convective ring while the inner eye wall, which had been associated with the maximum winds at peak intensity, was still visible, but rapidly decaying. This flight was at 850 hPa. If we assume that there was little difference between the wind speed maximum at 700 hPa and 850 hPa (which is usually the case in severe tropical cyclones) then it appears that Gilbert had become less intense than it was on 11 September 1988, even though the central pressure was 17 hPa lower. The lower central pressure may have been associated with a larger pressure gradient out to radius 150 km and beyond.

The reconnaissance data from *Gilbert* appear to suggest that for a given peak wind speed, the central pressure of a tropical cyclone may depend strongly on the radial profile of wind speed. This is consistent with theory as shown in the section on theoretical considerations.

Small tropical cyclones

***Ada* (1970).** In contrast to *Agnes*, *Ada* was an extremely small cyclone with gales extending only about 55 km from the centre – see Fig. 5. At 1100 UTC on 17 January 1970 the Mackay radar showed that *Ada* had an eye 28 km in diameter. The eye retained this diameter for several hours and then contracted to a diameter of 18 km by 1700 UTC. Over the period of contraction, the eye came only 13 km closer to the radar, suggesting that the contraction was real and not a manifestation of less attenuation of the radar signal, or the radar beam being directed at a significantly lower part of the eye. At 1700 UTC *Ada* was located over the Whitsunday Islands, the major island tourist destination in Australia. Notice the comparatively high pressure less than 100 km away (Fig. 5).

At 1500 UTC on 17 January 1970 the radar-observed centre of *Ada* was 9 km east of Hayman Island and the radar eye diameter was 22 km. The cyclone was 126 km away from the radar, which was set at zero elevation with the centre of the radar beam at 1 km elevation at that range. Without instrumentation, observers at Hayman Island estimated that the wind was around 50 m s^{-1}. *Ada* came closest (about 8 km) to Dent Island when the lowest pressure measured was 965 hPa and the

Fig. 5 **Mean sea-level pressure distribution while tropical cyclone Ada was near the Whitsunday Islands.**

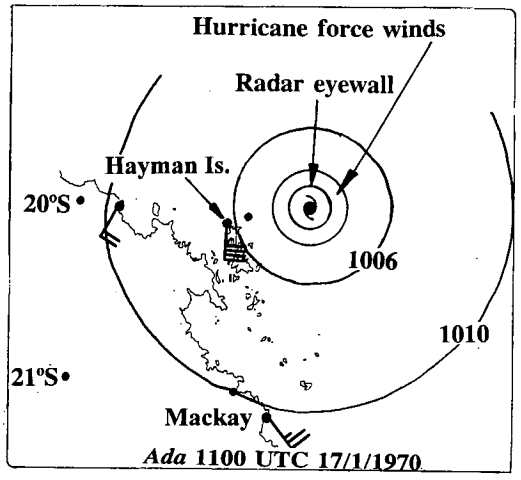

eye diameter was 20 km. On the mainland the coastal town of Airlie Beach recorded a minimum pressure of 962 hPa. The radar centre was 5 km from the town at 1930 UTC when it had an eye diameter of 22 km. The radar eye diameter was at a minimum of 20 km between 1630 UTC and 1830 UTC and from the above data it appears that the cyclone reached a minimum central pressure of nearly 960 hPa during this period.

As no instrumented wind observations were available in the vicinity of *Ada*, the effects of the wind must be examined to compare it with *Agnes*. In 1970 the coastal area which *Ada* passed through contained no large urban centre and was mostly farming or forest country. After its passage, the trees that were not blown over were stripped of all foliage and bark. The eye passed over nearby South Molle Island where almost all accommodation cabins were destroyed; one lady was killed in her cabin and her companion badly injured. On Hayman Island, two-thirds of the accommodation cabins were unroofed, with extensive damage to buildings. The cyclone's left front maximum wind zone passed directly over the Palm Bay resort on Long Island just before reaching the mainland. This resort was almost totally demolished, only isolated huts remained intact. Shute Harbour is the point of embarkation for the Whitsunday Islands and in those days consisted of a modern motel and a few houses. The eye passed directly over these and afterwards it reportedly looked like a city dump with the motel and houses torn apart. The main coastal centre in the region, Airlie Beach, was wrecked with 85 per cent of the houses destroyed. As *Ada* weakened overland, it passed to the south of Proserpine where 40 per cent of the buildings were unroofed or damaged. Fourteen lives were lost with the passage of *Ada*. Clearly, though of similar central pressure to *Agnes* as it reached the mainland, *Ada* was of greater intensity.

***Tracy* (1974), *Kathy* (1984).** Several other small cyclones are known to have seriously affected the coastline of northern Australia, including the Bowen cyclone of 1958, *Tracy* in Darwin in 1974 and *Kathy* in the Gulf of Carpentaria in 1984. The radius of maximum winds at landfall was 7 km for *Tracy* and about 10 km for *Kathy*. The radius of gales was only about 35 km for *Tracy* and about 65 km for *Kathy*.

In the case of both cyclones, anemometers failed as the eyewalls approached. The anemometer near *Tracy* recorded a peak gust of 60 m s^{-1} as it failed, while the anemometer near *Kathy* recorded a gust of 71 m s^{-1} just before failure. Accurate central pressures in the eyes of both cyclones were obtained; 940 hPa in *Kathy* and 950 hPa in *Tracy*. In *Tracy* an extreme pressure gradient of 5.6 hPa km^{-1} was observed near the radius of maximum wind (Bureau of Meteorology 1977). The peak gust recorded with *Tracy* occurred at 0305 local time just before the anemometer failed. Nearly half an hour elapsed before the eastern eyewall reached the anemometer just after 0330 local time. From the radar photograph at 0315 local time (Bureau of Meteorology 1977) the eastern eyewall was relatively clear of rain echoes, so arguably the anemometer was not in the cyclone's maximum wind zone around the time of its failure. Indeed the worst of the damage was reportedly between 3 and 4 km north and northwest of the anemometer over the suburbs of Nightcliff and Casuarina. This was the area through which the northern eyewall passed.

In the US Saffir-Simpson scale, the wind effects of a Category 4 cyclone are listed as -'Shrubs and trees blown down; all signs down. Extensive damage to roofing materials, windows and doors. Complete failures of roofs on many small residences. Complete destruction of mobile homes'. Many people are familiar with the photographs of damage at Darwin following *Tracy* and would agree that it easily fits this definition. The range of wind speeds covered by the US Category 4 cyclone corresponds with the range of wind speeds in the transition zone from Australian Category 4 to Category 5 cyclone.

The Dvorak (1984) technique of estimating intensity from satellite imagery suggested that *Kathy* was an exceptionally intense storm. Interpretations using the Dvorak technique leading up to landfall gave *Kathy* a

central pressure of 915 hPa to 925 hPa. This was based on the observation at 1800 UTC 20 April 1984 of a ring of deep convection with cloud tops colder than -77°C, surrounding a clear compact eye, a feature that is rarely observed. At landfall the cloud tops had warmed a little to be between -70°C and -63°C.

There is concern in the Queensland Tropical Cyclone Warning Centre that rigidly applying the central pressure wind relationship in Table 1 for storms like *Ada, Tracy* and *Kathy* would lead to serious underestimates of intensity.

***Inez* (1966).** Hawkins and Imbembo (1976) analysed aircraft reconnaissance data from this small intense hurricane. The lowest calculated central pressure was 927 hPa and the maximum flight level wind speed of 81 m s^{-1} was observed on the final pass at 2435 m elevation. This is similar to the maximum flight level (700 hPa) wind speed recorded in hurricane *Gilbert* (77 m s^{-1}), when the central pressure was 903 hPa. The question is whether this is evidence that the storms at this stage in their lives were of similar maximum intensity despite the 24 hPa difference in central pressure.

Medium-sized storms with varying wind profiles

***Alicia* (1983).** The central pressure of *Alicia* (as indicated by the 850 hPa heights in Fig. 12 of Willoughby (1990a)) continued to deepen until 0600 UTC 18 August 1983. The peak winds appear to have occurred six hours earlier from the wind information on this figure and from the isotach analyses accompanying Willoughby et al. (1985). As early as 1605 UTC 17 August 1983, the maximum winds were near peak intensity when the storm had a relatively high central pressure. This was associated with a peaked wind profile in a radial direction. From then on *Alicia* underwent a concentric eye cycle so that, at the time of the lowest central pressure, wind speeds above 35 m s^{-1} extended out to large radii. It appears that the flat profile of an extended band of near peak intensity winds which occurred around the time the outer eyewall started to supplant the inner eyewall contributed to a much lower central pressure than would occur with a narrow zone of similar wind speeds associated with a peaked profile.

***Kerry* (1979).** The first instrumented flight into a southern hemisphere tropical cyclone occurred in 1979 when the National Oceanic and Atmospheric Administration's WD-P3 research aircraft flew into slow-moving tropical cyclone *Kerry*. The aircraft flew into the cyclone on two consecutive days. On the first day *Kerry* had a central pressure of 955 hPa. Over the next 24 hours the central pressure rose by 10 hPa, although the maximum wind speeds increased at all levels (Black and Holland 1995). The low-level (540 m) wind profile in Figs 6(c) and 7(c) in Black and Holland (1995) can be seen to change from a flat to a peaked profile around the radius of maximum winds, particularly in the southwest quadrant. As seen in Figs 15 and 46 in Sheets and Holland (1981), the eyewall convection changed considerably over the 24 hours. The eyewall was not complete on either day, being echo-free in the northwest quadrant. On the second day a warm dry anomaly at middle levels in the southwest quadrant weakened as an upper trough approached the cyclone. Consequently there was much stronger reflectivity (>35 dBZ) in the southwest quadrant (where the strongest winds occurred) on the second day. In addition the diameter of the eye had shrunk from 90 km to around 60 km.

***Oliver* (1993).** Figure 6 shows the MSL isobar structure of severe tropical cyclone *Oliver* as it approached Lihou Reef Automatic Weather Station (AWS) in the Coral Sea during February 1993. *Oliver* was a medium-size storm and at the time had a large high pressure region to its south. Nearby, Willis Island weather radar showed a clearly defined eye throughout the period *Oliver* passed over the AWS, enabling an extremely accurate track to be derived. Using the AWS wind data a radial profile of the winds could be constructed.

Lihou Reef is a coral cay and the anemometer is located 10 m above the surface of the cay which is 6 m above MSL. The wind is averaged for 10 minutes every hour just before transmission time. There is no information on the maximum wind gust, or on wind speed over the remaining 50 minutes. The maximum wind recorded as *Oliver* passed very slowly over the AWS was 46 m s^{-1} and the radius of maximum wind was 28 km. The lowest pressure recorded in the eye was 950 hPa and the environmental pressure outside the cyclone's circulation was 1010 hPa.

Holland's (1980) analytical wind model assumes that gradient-wind balance holds. Locally we assume the winds at 10 m over the ocean in the intense core of a tropical cyclone are 75 per cent of the gradient wind. We arrived at this figure from analyses of past cyclonic winds at Willis Island Meteorological Station where the winds at 10 m were between 65 per cent and 85 per cent of the gradient wind. In the United States, Powell's (1980) planetary boundary-layer model typically reduces gradient level winds by 75 per cent to 85 per cent. However, these are one-minute averaged winds.

Using the 75 per cent relationship, the maximum gradient-level wind associated with *Oliver* was calculated to be 61.3 m s^{-1}. The Holland wind profile for *Oliver* based on this maximum gradient wind and the 60 hPa pressure drop was derived. This was then converted to a

Fig. 6 **Mean sea-level pressure distribution at 2300 UTC 6 February 1993. Locations of Willis Island and Lihou Reef are marked. Crosses mark position of latitudes 15°S and 20°S and longitudes 150°E.**

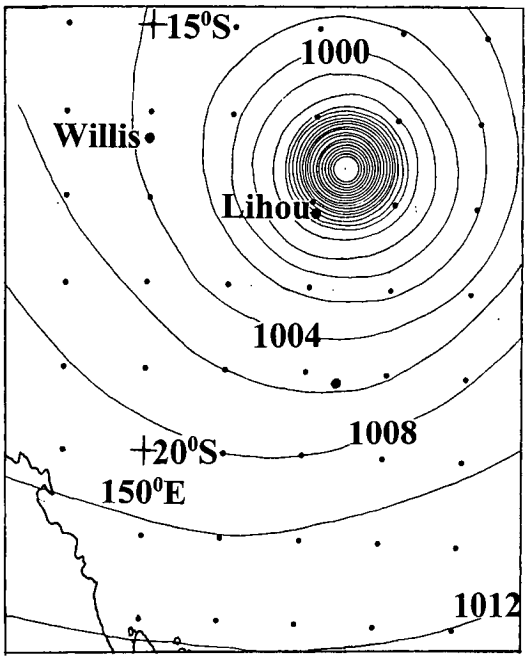

pseudo 10 m wind profile by reducing the gradient wind speeds by 25 per cent and this profile is plotted in Fig. 7. The B scaling parameter of Holland's used to obtain this profile was 1.96 which is towards the higher end of his scale (usually 1 to 2.5). The actual AWS wind observations are also plotted for comparison; both show a peaked wind profile in the radial direction.

The actual winds within 60 km of the centre on the left-hand side of Fig. 7 provide a good fit to the Holland 10 m profile. These winds were located on the poleward side of *Oliver* as it moved towards the strong high. During the six-hour period the eyewall passed over the AWS, *Oliver* was moving towards the south-southwest at only 1.2 m s^{-1} and the direction of the observed winds was from 160° and 170°. Subtracting the movement of the storm from the observed maximum wind of 1700/46 m s^{-1} gives a storm-relative maximum wind speed of 47 m s^{-1}.

As the northern eyewall passed over the AWS, *Oliver* was moving slightly faster (2.3 m s^{-1}) and the observed maximum wind there (280°/42 m s^{-1}) equates to a storm-relative wind speed of 43 m s^{-1}. The inner core convection was narrower on this equatorward side and

Fig. 7 **Radial profile of Holland's (1980) 0.75 gradient wind for a tropical cyclone with central pressure 950 hPa, radius of maximum wind 28 km, maximum gradient wind 61 m s^{-1} and environmental pressure 1010 hPa. Crosses mark wind speed observations at Lihou Reef for tropical cyclone *Oliver*.**

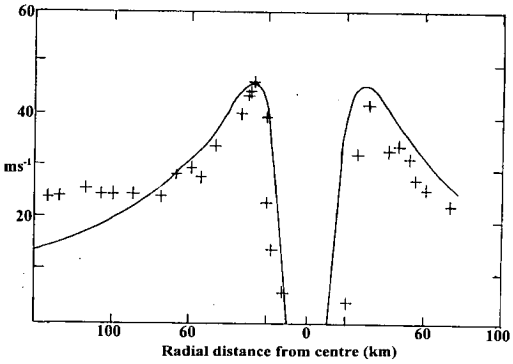

the winds dropped below storm force (24 m s^{-1}) at a radius of 74 km. On the poleward side, between the cyclone and the strong anticyclone, the storm-force winds extended out to 135 km.

The observed central pressure of 950 hPa was higher than expected from the eastern Australian central pressure–maximum wind relationship currently in use.

These observations indicate that the central pressure may depend also on the radial profile of the wind speed. The data from *Alicia* indicated such a relationship, while the second pass by reconnaissance aircraft over *Kerry* revealed an increase in both central pressure and maximum wind speed as the wind speed profile became more peaked in a radial direction. Rare oceanic AWS data from the eyewall of *Oliver* showed that it had a sharply peaked wind speed profile and a central pressure higher than expected from the operational central pressure–maximum wind speed relationship.

Effect of translation speed on maximum wind speed

New England Hurricane (1938)

An outstanding example of a rapidly translating cyclone is the 1938 New England Hurricane (Tannehill 1938; Pierce 1939) which accelerated rapidly towards Long Island as a major meridional upper trough amplified over the eastern United States. The hurricane was travelling northward at around 26 m s^{-1} when it reached the

coast of Long Island. An anemometer at Harvard University, which was over 120 km east of the centre, recorded a maximum five-minute wind of 54 m s^{-1} with gusts to 82 m s^{-1}. In contrast, Hartford, which was close to the centre but on its western side, recorded a maximum five-minute wind speed of 21 m s^{-1}. This clearly shows how the speed of translation added to the wind on the eastern side and reduced the wind to the west. More than 600 people were killed by the strong winds and the 10 m storm surge. The total damage bill was estimated at 400 million 1939 US dollars.

***Luis* (1995)**

On 11 September 1995 the vessel *Queen Elizabeth 11* (The Meteorological Office 1996) was near latitude 44°N and due south of the southeastern tip of Newfoundland. Hurricane *Luis* passed to the west of the ship in a northeasterly direction at 23 m s^{-1}. The ship's anemometer was hard up against the point of maximum deflection of 62 m s^{-1}. Five minutes later the anemometer was blown away. Sea-surface temperatures over these waters in summer are below 20°C, consequently, from DeMaria and Kaplan (1994), the maximum sustained storm-relative winds in hurricanes should not exceed 40 m s^{-1}. Although a rapidly moving storm may temporarily retain a higher intensity than the local sea-surface temperature would normally allow, the extreme sustained wind speeds of more than 62 m s^{-1} must have resulted from the rapid translation adding to the storm-relative winds.

An effect of these remarkable wind speeds was observed wave heights to 29 m which were verified by a nearby buoy which had peak wave heights of 30 m. Dysthe and Harbitz (1987) carried out analytical and observational studies of small systems such as polar lows and tropical cyclones generating very large waves. They found that rapid growth of waves occurred when a relationship existed between the movement of the cyclone (V) and the component of the wind velocity in the direction of motion of the cyclone (U). In particular, rapid growth occurs when $0.25 < V/U < 0.5$. The maximum observed sustained wind speed on the *Queen Elizabeth II* was at least 62 m s^{-1} and directed 30° to the right of the cyclone's path. Therefore $U = 62\cos 30 = 54$ m s^{-1} and $V/U = 0.42$ which is in the range for rapid growth of waves. It is generally accepted that the largest wave height ever observed was 34.1 m by a qualified observer aboard the *USS Rampago* in a typhoon in 1933. This wave was measured by triangulation and doubters have reexamined the mathematics of that incident ever since it was reported. The observation of a 30 m wave height, therefore, represents an extreme event. It follows that the wind field of *Luis* must have been extremely efficient in producing waves and that V/U must have been located near the centre of the window for rapid growth of waves ($V/U = 0.375$). For $V = 23$ m s^{-1} this corresponds to $U = 61$ m s^{-1} and a maximum sustained wind speed of $61/\cos 30 = 70$ m s^{-1} on board the *Queen Elizabeth II*. Therefore the observation of sustained wind speeds greater than 62 m s^{-1} on the ship is supported by the recorded extreme wave heights in the area.

Intense, rapidly moving cyclones in the southern hemisphere include that described by Foley and Hanstrum (1994) in Western Australia, and tropical cyclone *Giselle* (1968), with a modest central pressure of 978 hPa, which caused 51 deaths and widespread damage as it moved quickly over the North Island of New Zealand in 1968.

Theoretical considerations

The foregoing observations point to a relationship between central pressure and storm intensity that depends, *inter alia*, on storm size and translation speed. We show below that such a dependence is in line with basic dynamical principles.

Effects of translation speed on the pressure–intensity relationship

Consider a barotropic vortex with an axisymmetric vorticity distribution embedded in a uniform zonal air stream $\bar{U}$ on an f-plane. In a fixed, rectangular coordinate system (x, y), with x pointing eastwards and y pointing northwards, the streamfunction for the flow has the form:

$$\psi(x,y) = -\bar{U}y + \psi'(r) \qquad ...1$$

where $r^2 = (x - \bar{U}t)^2 + y^2$. The corresponding velocity field is:

$$\mathbf{u} = (\bar{U}, 0) + (-\partial\psi' / \partial y, \partial\psi' / \partial x) \qquad ...2$$

The relative vorticity distribution, $\zeta = \nabla^2\psi'$, is symmetric about the point $(x - \bar{U}t, 0)$, which translates with speed $\bar{U}$ in the x-direction. However, neither the streamfunction distribution $\psi(x, y)$, nor the pressure distribution $p(x, y)$, are symmetric and, in general, the locations of the minimum central pressure, maximum relative vorticity, and minimum streamfunction (where $\mathbf{u} = \mathbf{0}$) do not coincide. In particular, there are three important deductions from Eqn 2:

- the total velocity field of the translating vortex is not symmetric;
- the maximum wind speed is simply the arithmetic sum of $\bar{U}$ and the maximum tangential wind speed of the symmetric vortex, $V_m = (\partial\psi' / \partial r)_{max}$

- the maximum wind speed occurs on the right-hand side of the vortex in the direction of motion in the northern hemisphere and on the left-hand side in the southern hemisphere.

The last result is obtained below.

Figure 8 shows an example of the vorticity, streamfunction and wind speed distribution for a typical tropical cyclone-scale vortex, the one used by Smith et al. (1990), translating in a uniform westerly current of 10 m s^{-1}. The maximum tangential velocity is 40 m s^{-1}.

Because the vorticity field is Galilean invariant while the pressure field and streamfunction fields are not, it is convenient to define the vortex centre as the location of maximum relative vorticity and to transform the equations of motion to a coordinate system $(X, Y) = (x - \bar{U}t, y)$ whose origin is at this centre. In this frame of reference, the streamfunction centre is at the point $(0, Y_s)$, where:

$$\bar{U} - \Phi(Y_s)Y_s = 0 \qquad ...3$$

and $\Phi(R) = \psi'(R)/R$. This point is to the left of the vorticity centre in the direction of motion in the northern hemisphere. In the moving coordinate system, the momentum equations may be written in the form:

$$\nabla p = \rho\Phi(\Phi + f)[X, Y] + \rho f[0, U] \qquad ...4$$

The derivation is outlined in the appendix. The minimum surface pressure occurs where $\nabla p = 0$, which from Eqn 4 is at the point $(0, Y_p)$ where:

$$Y_p\Phi(Y_p)[\Phi(Y_p) + f] = f\bar{U} \qquad ...5$$

We show that, although Y_p and Y_s are not zero and not equal, they are for practical purposes relatively small.

Consider the case where the inner core is in solid body rotation out to the radius r_m, of maximum tangential wind speed v_m, with uniform angular velocity $\Omega = v_m/r_m$. Then $\psi'(R) = \Omega R$ and $\Phi = \Omega$. It follows readily that $Y_s/r_m = \bar{U}/v_m$ and $Y_p/r_m = \bar{U}/(v_m Ro_m)$, where $Ro_m = v_m/(r_m f)$ is the Rossby number of the vortex core. This number is large compared with unity in a tropical cyclone. Taking typical values: $f = 5 \times 10^{-5}$ s^{-1}, $\bar{U} = 10$ m s^{-1}, $v_m = 50$ m s^{-1}, $r_m = 50$ km, $Ro_m = 20$ and $Y_s = 10$ km, $Y_p = 0.5$ km, the latter being much smaller than r_m. Clearly, for weaker vortices (smaller v_m), and/or stronger basic flows (larger $\bar{U}$), the values of Y_s/r_m and Y_p/r_m are larger and the difference between the various centres may be significant.

Fig. 8 **Contour plots of (a) total wind speed, (b) relative vorticity, and (c) streamlines, for a vortex with a symmetric relative vorticity distribution and maximum tangential wind speed of 40 m s^{-1} in a uniform zonal flow with speed 10 m s^{-1} on an f-plane. The maximum tangential wind speed occurs at a radius of 100 km (for the purpose of illustration). The contour intervals are: 5 m s^{-1} for wind speed, 2 x 10^{-4} s^{-1} for relative vorticity and 1 x 10^{-4} $m^2 s^{-1}$ for streamfunction.**

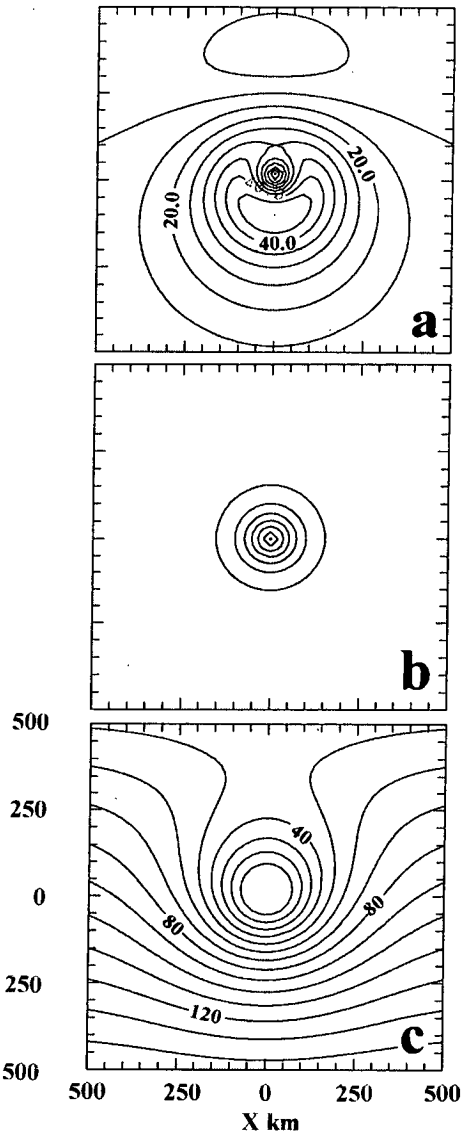

Effects of vortex size on the pressure – intensity relationship

For mathematical simplicity we consider a piecewise-continuous symmetric vortex with a tangential wind profile $v(r)$ given by:

$$v(r) = \begin{cases} v_m \dfrac{r}{r_m} & \text{for } 0 \le r \le r_m \\ v_m \Phi(r/r_m, r_0) & \text{for } r_m \le r \end{cases} \qquad ...6$$

where Φ is some function which is positive for all r, equals unity at $r = r_m$ and decays monotonically to zero as $r \to \infty$. This allows us to vary the outer circulation independently from that in the inner core. The parameter r_o is chosen to characterise the rate of decay of the vortex with radius, i.e. the scale of its outer circulation; we assume that $\partial\Phi/\partial r_o > 0$ so that the outer vortex strength increases with r_o. The profile Φ should have the additional properties that the integrated kinetic energy of the vortex $\int_0^\infty 2\pi r(1/2\ \rho v^2)dr$ and the integrated angular momentum $\int_0^\infty 2\pi r(\rho r v)dr$ are finite, and it should be inertially stable*.

Let us assume that the vortex is in gradient wind balance so that the pressure p varies with radius according to the equation

$$\frac{dp}{dr} = \rho\left(\frac{v^2}{r} + fv\right) \qquad ...7$$

This is a good assumption in tropical cyclones above the boundary layer (Willoughby 1990b); later we consider the effects of boundary-layer friction. Substituting for $v(r)$ from Eqn 6 and integrating Eqn 7 with respect to r in the two ranges $(0, r_m)$ and (r_m, ∞) gives

$$p(\infty) - p(r_m) = 1/2\ \rho v_m^2 \int_{r_m}^{\infty}\left(\frac{\Phi^2}{r} + f\Phi\right)dr \qquad ...8$$

and

$$p(r_m) + p(0) = 1/2\ \rho v_m^2\left[1 + \frac{1}{Ro_m}\right] \qquad ...9$$

whereupon

$$p(\infty) - p(0) = 1/2\ \rho v_m^2\left[1 + \frac{1}{Ro_m} + \int_{r_m}^{\infty}\left(\frac{\Phi^2}{r} + f\Phi\right)dr\right] \qquad ...10$$

Note from Eqn 10 that the pressure difference between the far environment and the storm centre scales with ρv^2_m. Moreover, for a fixed v_m it increases with increasing vortex scale r_O, because the integral on the right-hand-side of Eqn 10 increases† with Φ. In other words, for the same vortex intensity, the central pressure of smaller storms is higher than for larger storms. Thus, on the reasonable assumption that gradient-wind balance exists, there cannot be a one-to-one correspondence between storm intensity and central pressure.

As a slight generalisation of the foregoing profile, it is interesting to enquire what the effect would be if there is a region of dead calm in the inner part of the vortex core (inside a radius a), a situation which may or may not be the case in reality. This can easily be incorporated by considering the tangential wind profile

$$v(r) = \begin{cases} 0 & \text{for } 0 \le r \le a \\ v_m\ \dfrac{(r-a)}{(r_m - a)} & \text{for } a \le r \le r_m \\ v_m\ \Phi\ (r/r_m, r_0) & \text{for } r_m \le r \end{cases} \qquad ...11$$

which has the same outer structure (for $r > r_m$) as Eqn 1. With this profile, the gradient wind Eqn 7 gives

$$p(r_m) - p(a) = 1/2\ \rho v_m^2\left[\frac{r_m - 3a}{r_m - a} + \frac{2a^2}{(r_m - a)^2}\ln\frac{r_m}{a} + \frac{1}{Ro_m}\left(1 - \frac{a}{r_m}\right)\right] \qquad ...12$$

and

$$p(a) - p(0) = 0 \qquad ...13$$

The outer pressure difference $p(\infty) - p(r_m)$ given by Eqn 8 remains unchanged. The radial pressure profiles are shown in Fig. 9 for various values of a with a typical outer profile. They indicate that, if for any reason the winds were dead calm within a radius a of the vortex centre, then for the same r_m and v_m, the central pressure would be higher than for a vortex where the tangential winds extend to the centre.

Effects of friction

The foregoing analysis neglects the effects of surface friction, one of which is to reduce the tangential wind speed in a shallow boundary layer, typically on the order of five hundred metres deep in a hurricane. However, friction has little effect on the strength of the radial pressure gradient, which is comparable in the boundary layer to that in the free atmosphere above. The reduction in the Coriolis and centrifugal forces associated with the reduction in tangential wind speed leads to a breakdown of gradient wind balance in the boundary layer and in a cyclonic vortex leaves a net radially inward pressure gradient. This drives an inward radial flow in the boundary layer with maximum speed comparable in magnitude, but typically less than the maximum tangential wind speed above the boundary layer (see e.g. Smith 1968; Bode and Smith 1975). The presence of this radial wind component and the reduced tangential wind component will modify the results in the two preceding sections when applied to the near-surface flow. Clearly a particular central pressure will have to be associated with a lower maximum surface wind speed than that above the boundary layer as was done with *Inez* and

* This means that the vortex is stable to axisymmetric overturning motions and requires that the quantity $I^2 = (1/r\ \partial(rv)/\partial r + f)(2v/r + f)$ is everywhere positive (see e.g. Eliassen (1951).

† Mathematically, $\partial/\partial r_O\ (p(\infty) - p(0)) = 1/2\ \rho v_m^2\ [\int_{r_m}^{\infty}(2\Phi/r + f)\ \partial\Phi/\partial r_O\ dr] > 0$ because $\Phi > 0$ and $\partial\Phi/\partial r_O > 0$.

Fig. 9 **Profiles of $p(r) - p(\infty)$ calculated using Eqn 11 for values of a ranging from 0 km to 40 km in steps of 10 km for the case where v_m = 50 m s^{-1}, r_m = 50 km. A typical radial variation of $p(r)$ outside the radius of maximum winds is shown. The central pressure and hence the value of $|p(0) - p(\infty)|$ decreases as a increases on account of the reduction in the value of $|p(0) - p(r_m)|$.**

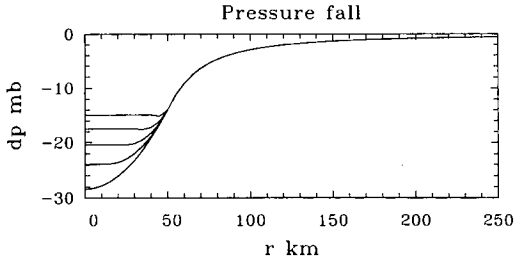

Gilbert earlier. Nevertheless, the dependence of the central pressure – maximum wind relationship on storm size and translation speed may be expected to remain.

The presence of storm translation on the boundary-layer structure and the flow asymmetries that arise therein is a further complication (Shapiro 1983), but is unlikely to affect the general conclusions reached here. Careful consideration of such asymmetries would be required, however, to determine the possible influence of the radial wind structure on the central pressure – maximum wind relationship as suggested by the observations of hurricane *Luis* (1995) described above; such an analysis is beyond the scope of the present work.

Summary

Tropical cyclone forecasters in Australia are required to advise the central pressure of tropical cyclones in warnings and bulletins. This study followed recommendations from the 1996 Bureau of Meteorology Tropical Cyclone Review Conference and was initiated to document situations when, using established pressure-wind relationships, the central pressure of a tropical cyclone misrepresents its maximum wind speed and to explore the variable relationship between central pressure and maximum wind speed.

Some tropical cyclone forecasters are concerned that the central pressure in very small intense cyclones underestimates their intensity. Currently, at the Joint Typhoon Warning Centre in Guam, guidance to forecasters indicate that midget cyclones (radius of gales of 111 km or less) can sustain hurricane-force winds with central pressures 20 to 25 hPa higher than larger storms. Where observations have been available for these small storms they have been found to have a very sharp peaked wind profile in the radial direction. Average-sized storms were also shown to have higher central pressures than expected when they had a sharply peaked wind profile in the radial direction. From evidence available to date in the northeast Australian region, the Dvorak technique is still a very useful guide to intensity, with the cloud-top temperature patterns being closely related to maximum wind speeds, particularly in the developing phase.

Large, intense cyclones appear to have much lower central pressures than small cyclones of similar intensity. This is especially evident when they are in the midst of a concentric eye cycle. Then the radial wind profile becomes flat and the wind speed is close to the maximum to a large radius. However, near peak intensity, large intense cyclones also have strongly peaked wind speed profiles close to the centre, outside of which is a flat profile associated with the outer eye. *Gilbert* had an extremely tight inner eye at peak intensity with an echo-free area of 7 km radius. Giant super-typhoon *Tip* had a satellite eye diameter of only 24 km at maximum intensity. However these large storms had gales out to large radii with a considerable drop in pressure even outside the inner core. The pressure has been observed to drop up to 20 hPa across the area of gales outside the core of large cyclones. The question then is whether large cyclones have lower central pressures than equally intense small storms throughout the concentric eye cycle. If it was valid to equate *Inez* and *Gilbert* above then this provides one example to support the hypothesis that small cyclones always have higher central pressures than equally intense large storms.

The translation speed of a storm adds to the mean tangential wind component to increase the total wind without affecting the central pressure. With rapidly moving storms, this effect can be substantial, as in the case of *Luis* discussed above. Although *Luis* was probably a Category 3 cyclone, the winds were those of a high Category 4 intensity storm.

We have shown that the foregoing observations can be explained in terms of simple dynamical principles.

Acknowledgments

We thank David Bernard, Rex Falls and two anonymous referees for their helpful reviews. The second author's contribution to this research was supported by the US Office of Naval Research through Grant No. N00014-95-1-0394.

References

Black, M.L. and Willoughby, H.E. 1992. The concentric eyewall cycle of Hurricane Gilbert. *Mon. Weath. Rev., 120*, 947-57.

Black, P.G. and Holland, G.J. 1995. The boundary layer of Tropical Cyclone Kerry (1979). *Mon. Weath. Rev., 123*, 2007-28.

Bode, L.M. and Smith, R.K. 1975. A parameterization of the boundary layer of a tropical cyclone. *Bound. Lay. Met., 8*, 3-19.

Brand, S. 1972. Very large and very small typhoons of the Western North Pacific. *J. met. Soc. Japan, 50*, 332-41.

Bureau of Meteorology 1977. *Report on Cyclone Tracy December 1974*. Bur. Met., Australia.

DeMaria, M and Kaplan, J. 1994. Sea surface temperatures and the maximum intensity of Atlantic tropical cyclones. *Jnl climate, 7*, 1324-34.

Dunnavan, G.M. and Diercks, J.W. 1980. An analysis of super Typhoon Tip (October 1979). *Mon. Weath. Rev., 108*, 1915-2023.

Dvorak, V.F. 1984. Tropical Cyclone Intensity Analysis Using Satellite Data. *NOAA Technical Report NESDIS 11*, 45pp.

Dysthe, K.B. and Harbitz, A. 1987. Big waves from polar lows. *Tellus 39A*, 500-8.

Eliassen, A. 1951. Slow thermally or frictionally controlled meridional circulation in a circular vortex. *Astrophys. Norv., 5*, 19-60.

Eyre, A.L. 1989. Hurricane Gilbert: Caribbean record-breaker. *Weather, 44, no. 4*, 160-4.

Foley, G.R. and Hanstrum, B.N. 1994. The capture of tropical cyclones by cold fronts off the west coast of Australia. *Weath. forecasting, 9*, 577-92.

Hawkins, H.F. and Imbembo, S.M. 1976. The structure of a small intense hurricane- Inez 1966. *Mon. Weath. Rev., 104*, 418-42.

Holland, G.J. 1980. An analytic model of the wind and pressure profiles in hurricanes. *Mon. Weath. Rev., 108*, 1212-18.

Merrill, R.T. 1984. A comparison of large and small tropical cyclones. *Mon. Weath. Rev., 112*, 1408-18.

Pierce, C.H. 1939. The meteorological history of the New England Hurricane of Sept. 21 1939. *Mon. Weath. Rev., 67*, 237-85.

Powell, M.D. 1980. Evaluations of diagnostic marine boundary layer models applied to hurricanes. *Mon. Weath. Rev., 108*, 757-66.

Shapiro, L.J. 1983. The asymmetric boundary layer flow under a translating hurricane. *J. Atmos. Sci., 40*, 1984-98.

Shea, D.J. and Gray, W.M. 1973. The hurricane's inner core region. I. Symmetric and asymmetric structure. *J. Atmos. Sci., 30*, 1544-64.

Sheets, R.C. and Holland, G.J. 1981. Australian tropical cyclones Kerry and Rosa, 1979. *NOAA Tech. Memo. ERL-AOML-46*, Atlantic Oceanographic and Meteorological Laboratories, Miami, Fl., 138pp.

Smith, R.K. 1968. The surface boundary layer of a hurricane. *Tellus, 20*, 473-84.

Smith, R.K., Ulrich, W. and Dietachmayer, G. 1990. A numerical study of tropical cyclone motion using a barotropic model. Part 1. The role of vortex asymmetries. *Q. Jl R. met. Soc., 116*, 337-62.

Subbaramayya, I. and Fujiwhara, S. 1979. A note on the relationship between maximum surface wind and central pressure in tropical cyclones in Western North Pacific. *J. met. Soc. Japan, 57*, 358-60.

Tannehill, I.R. 1938. Hurricane of September 16 to 22, 1938. *Mon. Weath. Rev., 66*, 286-8.

The Meteorological Office 1996. Hurricane Luis, the Queen Elizabeth II and a rogue wave. *The Marine Observer, 66*, 134-7.

Willoughby, H.E. 1990a. Temporal changes of the primary circulation in tropical cyclones. *J. Atmos. Sci., 47*, 242-64.

Willoughby, H.E. 1990b. Gradient wind balance in tropical cyclones. *J. Atmos. Sci., 47*, 265-74.

Willoughby, H.E., Jorgensen, D.P., Black, R.A. and Rosenthal, S.L. 1985. Project STORMFURY: A scientific chronicle 1962-1983. *Bull. Am. met. Soc., 66*, cover and 505-14.

Appendix

The momentum equation for the symmetric vortex in a uniformly moving coordinate system

The two-dimensional Euler equations of motion in the fixed frame of reference on an f-plane have the form

$$\frac{\partial u}{\partial t} + u\frac{\partial u}{\partial x} + v\frac{\partial u}{\partial y} - fv = -\frac{1}{\rho}\frac{\partial p}{\partial x} \qquad \text{...A1}$$

$$\frac{\partial v}{\partial t} + u\frac{\partial v}{\partial x} + v\frac{\partial v}{\partial y} + fu = -\frac{1}{\rho}\frac{\partial p}{\partial y} \qquad \text{...A2}$$

using the earlier notation. With the coordinate transformation (x,y,t) to $(X,Y,T) = (x - \bar{U}t, y, t)$, the derivatives become

$$\begin{pmatrix} \frac{\partial}{\partial t} \\ \frac{\partial}{\partial x} \\ \frac{\partial}{\partial y} \end{pmatrix} = \begin{pmatrix} 1 & -\bar{U} & 0 \\ 0 & 1 & 0 \\ 0 & 0 & 1 \end{pmatrix} \begin{pmatrix} \frac{\partial}{\partial T} \\ \frac{\partial}{\partial X} \\ \frac{\partial}{\partial Y} \end{pmatrix} \qquad \text{...A3}$$

In this reference frame, the streamfunction for the translating vortex in the section on theoretical considerations has the form

$$\psi = -\bar{U}y + \psi'(x - \bar{U}t, y)$$

but the frame of reference located at the vortex centre (X=Y=0) and moving at speed $\bar{U}$ in the x-direction it reduces to $\Psi = \Psi(R)$, where $R^2 = X^2 + Y^2$. The velocity components (U,V) in the moving frame are given by

$$(U,V) = \left(-\frac{\partial \Psi}{\partial X}, \frac{\partial \Psi}{\partial Y}\right) = \frac{\partial \Psi}{\partial R}\left(-\frac{\partial R}{\partial Y}, \frac{\partial R}{\partial X}\right) = \Phi(R)(-Y,X)$$

where $\Phi(R) = (1/R)(\partial\Psi/\partial R)$. Note that $u = U + \bar{U}$ and $v = V$. Substituting these last two relations into Eqns A1 and A2 and using Eqn A3 it follows readily that for the moving vortex, the momentum equation reduces to:

$$\nabla p = \rho\Phi(\Phi + f)[x,y] - f[0,U] \qquad \text{...A4}$$